TRENDS IN SCIENCES 2025; 22(10): 10404
https://doi.org/10.48048/tis.2025.10404 RESEARCH ARTICLE

Study the Optical and Electrical Properties of Gold Nanoparticles Deposited on Porous Silicon

Taghreed Mahmood Younus[1], Mazin Ahmed Abed[2], Mahmood Ahmed Hamood[2] and Ghazwan Ghazi Ali[1,*]

[1]Department of Physics, College of Education for Pure Science, University of Mosul, Mosul 41002, Iraq
[2]Department of Physics, College of Science, University of Mosul, Mosul 41002, Iraq

([*]Corresponding author's e-mail: dr.ghazwan39@uomosul.edu.iq)

Received: 18 April 2025, Revised: 21 May 2025, Accepted: 1 June 2025, Published: 20 July 2025

Abstract

Gold nanoparticles have been vast attractive attention materials due to unique of the electronic applications. In this paper, the colloidal of gold nano layer has been achieved by laser ablation at high power laser (200, 300 and 400 mJ) and then, deposited on porous silicon substrate using electrochemical etching method. The performance and characterization of Au/porous silicon samples have been examined. The results confirmed that the PSi has network like sponge shape structure with uniform distribution. The absorption spectra increase with increasing power laser and the strong peaks were found to be (542, 546 and 550 nm) at (200, 300 and 400 mJ), respectively. This is due to surface plasmon phenomena. The photoluminescence of gold nanostructures revealed the peak position was shifted to the long wavelength(redshift) with increasing power laser. Current – voltage measurements of AuNPs/PSi device exhibit that the current values increase with increasing power laser. Gold nanoparticles deposited on porous silicon can be can be achieved for optoelectronic devices.

Keywords: Laser ablation, PSi, Gold nanoparticles, SEM, Photoluminescence

Introduction

Gold nanoparticles have been received a numerous attention in both fabrication and application fields. For example, the important properties of the nanoparticles such as, electrical, optical and magnetic properties can be highly modified by manipulating in nanoparticle size [1-3]. Au nanoparticles recently gaining vast attention owing to their wide range of applications due to the unique of the optical and electrical properties making it a good candidate for cancer diagnosis and photo-thermal therapy [4]. In fact, gold nanoparticles have strongly interaction with light due to the electrons in the conduction band as well as have unique efficiency for light absorbing [5]. This occurs due to surface plasmon resonance (SPR), which makes the scattering and absorption spectra of Au nanoparticles higher than the identically sized non-plasmonic nanostructures [6]. Au nanoparticles of optical properties can be modified by

adjusting the particle shape and size near the particle surface [7]. On the other hand, laser ablation is one of simplest method for ablating solid target materials. In this technique, power laser beam is focused on a specific area of the target to evaporating light absorption material [8]. In fact, high purity nanomaterials can be estimated by laser ablation due to the purity of the target and the ambient material which is usually gas or liquid [9]. In 2013, Tengku *et al*. studied the optical absorption and photoluminescence of Au nanoparticles on porous silicon. They found a significant blue shift with decreasing AuNP size due to localized plasmon resonances [10]. In 2017, Falah *et al*. prepared and studied Au nanoparticles for nanomedicine application. Their results showed that

AuNPs has excellent antibacterial sensitivity [11]. In 2018, Uday *et al*. studied deposition of Au nanoparticles by laser ablation on PSi for gas sensor, They concluded that the electrical measurements and sensitivity of CO_2 gas were measured to AuNPs/PSi, they found that Gold nanoparticles play key role to improve this characteristics [12]. In 2019, Ibrahim *et al*. reported Gold deposited porous silicon as surface-enhanced Raman scattering, this study illustrates that the SERS improvements depend on the gold film thickness and the roughness surface of the Au /PSi [13]. There are rarely focused studies on the comparison between n-type porous silicon and p-type porous silicon samples of various laser ablation power on the physical properties of Au nanoparticles. In this article, we study the deposition of the Au nanoparticle created by laser ablation with different power laser on PSi substrate layer. The high lattice-match between Au and PSi makes it a high quality device with negligible defects. The experimental characterization in this study were done by SEM, UV-Vis Spectroscopy, I-V measurements and Photoluminescence.

Materials and methods

Silicon wafers of n-type (111) and p-type (111) with resistivity (0.01 - 2 Ω.cm) were used. The current density was applied at 50 mA/cm ^{2}. Porous silicon substrate was prepared by electrochemical etching using Tungsten source of 100 MW/cm^2. Etching time taken for 30 min and generated by DC power supply. The samples were immersed in 25 %HF acid concentration with ethanol. Anodized Teflon cell of a rubber O-ring diameter about 2.5 cm^2 is used to touch the beneath PSi layer. the first electrode is a steel foil put under the Si layer and the second electrode is made of Au as it shows in **Figure 1**. On the other hand, the Au nanoparticles (Au NPs) were prepared using laser ablation method. Gold metal with high purity was used and immersed in water then directly bombarded with high power value Nd:YAG laser emission at 1064 nm with various energy namely (200, 300 and 400 mJ). Au nanoparticles carried out using laser ablation in a liquid at pulse duration 3 ns and repetition rate of 6 kHz with 3.7 mm spot size. The number of the pulses kept 200 and 14 cm focal length lens was used in order to focus the laser beam as it depicted in **Figure 2**.

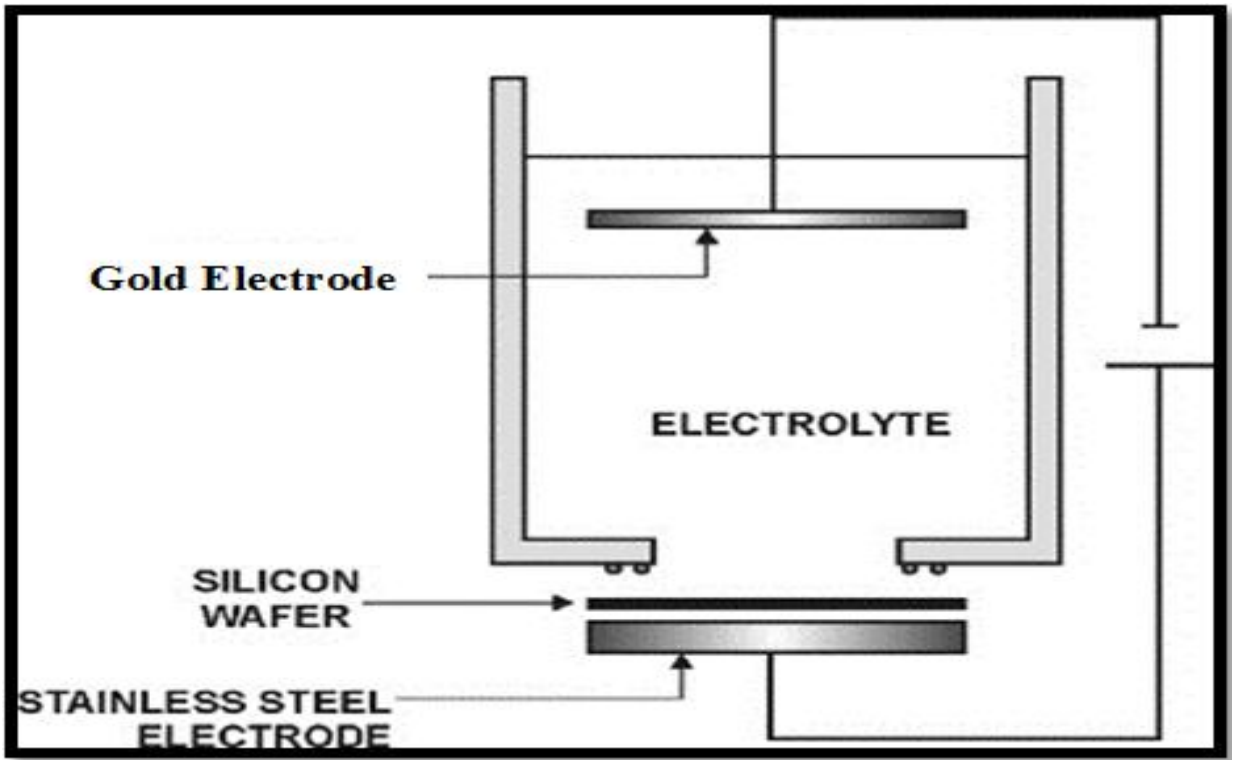

Figure 1 Set up of electrochemical etching.

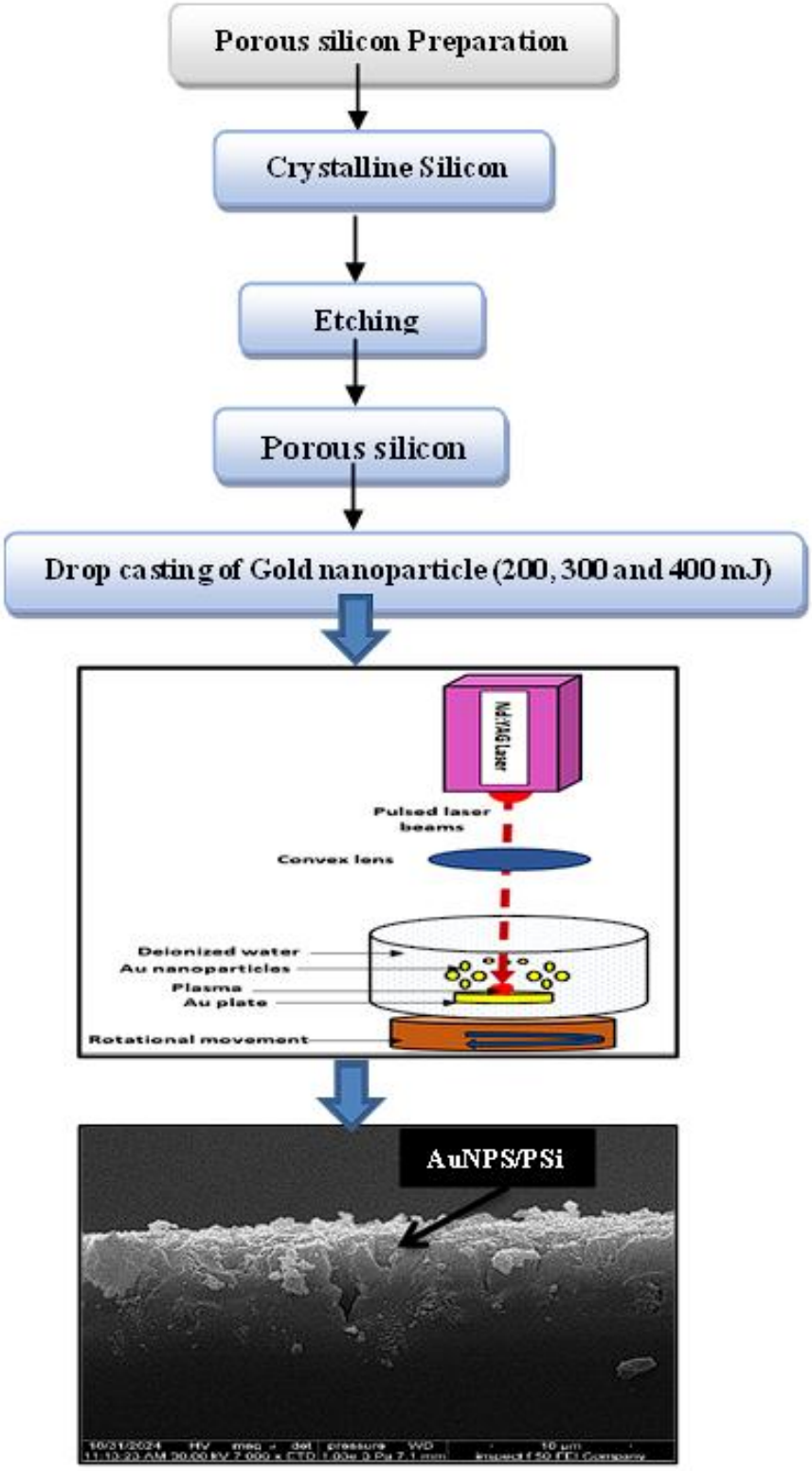

Figure 2 Diagram of laser ablation process.

Results and discussion

Scanning electron microscope (SEM)

Figure 3 shows the top- view of high resolution of Au nanoparticles embedded on porous silicon at different power laser 200, 300 and 400 mJ at etching time 30 min. The SEM images reveal that the PSi has sponge-like structure due to the chemical dissolution in the walls separating between the pores and then to easy excess of holes at the surface as **Figure 3(a)**. Furthermore, the gold nanoparticles embedded on

porous silicon surface exhibit major impact when the power laser increased [14,15]. The grain size of Au increases with increasing power laser due to aggregation and formation of Au nanoparticles during preparation process. The formation of nano- size is homogenous distribution with gradually increasing power laser [16]. The average pore- diameter of gold nanoparticles was found to be (15 - 57 nm) as **Figures 3(b) - 3(d)**.

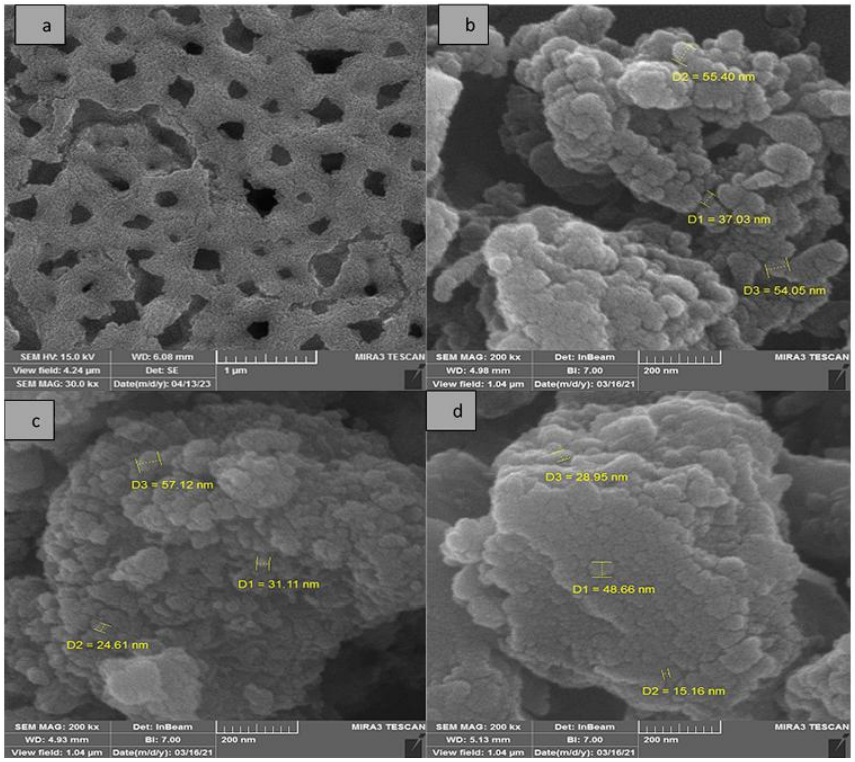

Figure 3 Images of SEM (a) fresh porous silicon at etching time 30 min, (b) Au/porous silicon at power energy 200 mJ, (c) Au/porous silicon at power energy 300 mJ, (d) Au/porous silicon at power energy 400 mJ.

UV- spectrophotometer

The optical properties of AuNP was studied using spectrophotometer analysis as a function of wavelength delivers evidence for available electronic states in the sample. **Figure 4** illustrates the absorbance spectra of colloidal Au nanoparticles for different laser energy (200, 300 and 400 mJ). It is obviously, that the absorption curves reveal an absorption band located between 542 - 550 nm. This is due to surface plasmon resonances (SPR) and quantum confinement indicating the formation Au nanoparticles [17]. The results confirmed that the AuNPs has spherical shape. Furthermore, the intensity of absorption peak depends on the number of nanoparticles [18]. The peak wavelength is red shift due to the localized electric field intensity increases with increasing of radius of AuNPs. This is enhanced field distribution of Au NPs/PSi[19]. **Figures 5(a) - 5(b)** show the transmission curves of AuNPs/PSi device for n-type and p-type porous silicon, respectively. The results show that transmission spectra reduce with the laser power which is due to the SPR spectrum of the free electrons [20]. The values of transmission of n-type porous silicon at 550 nm range from 65% to 80% whereas, for p-type porous silicon it range from 75% to 90%. This became more widely distributed around the surfaces of p- type porous silicon compared to n-type porous silicon. This indicated that the AuNPs has diffused with uniform sizes inside the PSi nanostructures, thus, larger sizes of AuNPs were produced. The energy gap can be calculated from the fundamental absorption by plotting $(\alpha h\nu)^2$ against photon energy $(h\nu)$ for different power laser (200, 300 and 400 mJ) as shown in **Figures 6(a) - 6(d)**. The energy gap (E_g) can be calculated by formula:

$$\alpha h\upsilon = b(h\upsilon - Eg)^n \quad (1)$$

where b is constant, n represents direct and indirect transition and its value are 1/2 and 2, respectively, hυ refers to photon energy and α is the absorption coefficient. The results indicate the values of Eg decrease with laser power, this is attributed to the increase of particle size of AuNPs and occurs expanding into the pores due to the absorption depend on the concentration of the nanoparticles [21]. The values of energy gap were found to be 2.12, 2.11 and 2.09 eV for n-type porous silicon at 200, 300 and 400 mJ, respectively, compared to 2.17, 2.15 and 2.13 eV for p-type porous silicon at 200, 300 and 400 mJ, respectively. **Table 1** shows strong peaks and wavelength of Au nanoparticles at different laser power. It can be seen the SPR spectrum was shifted toward longer wavelength when the particle size increased due to the absorption position depends on free electrons and the laser power, it may be due to the presence of small fragments in the colloidal solution during the laser ablation process leading to enhance the collision process between atoms and vapor ions [22]. Those results exhibit that the optimization of the gold nanoparticles can be significantly developed by controlling the power laser during the ablation process of the Au target [23].

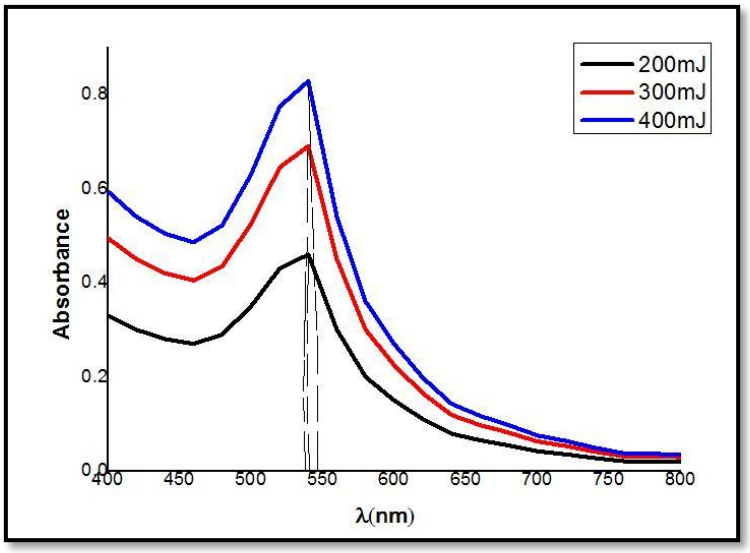

Figure 4 Absorbance spectra of Au nanoparticles of laser ablation energy of 200, 300 and 400 mJ.

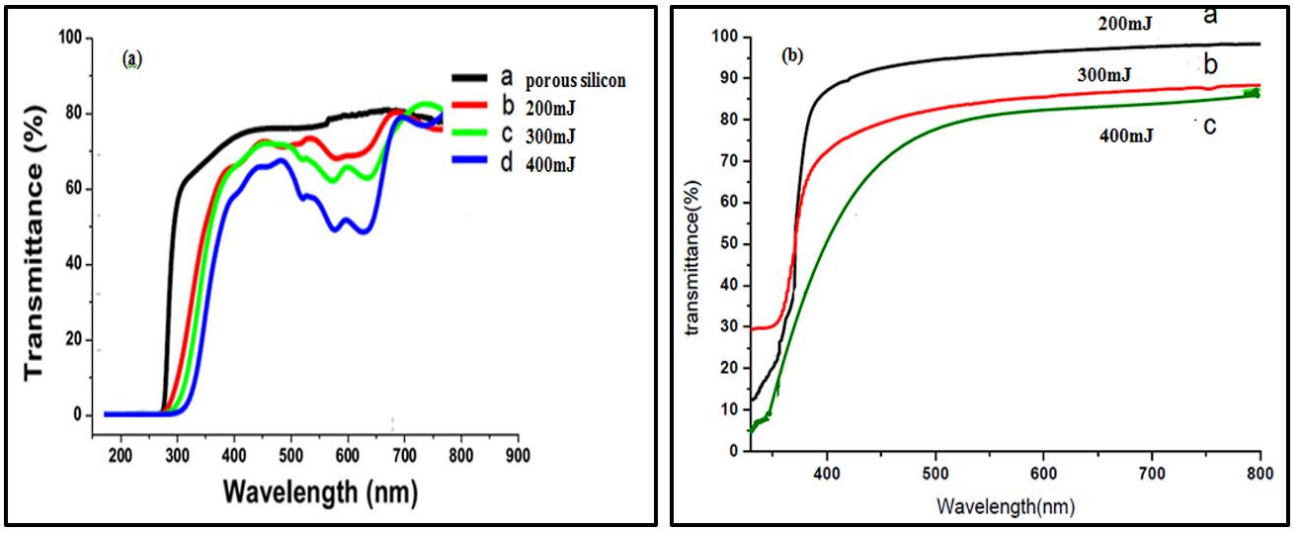

Figure 5 Transmittance spectra of AuNPs/PSi of laser ablation energy of 200, 300 and 400 mJ 5(a) for n-type 5(b) p-type.

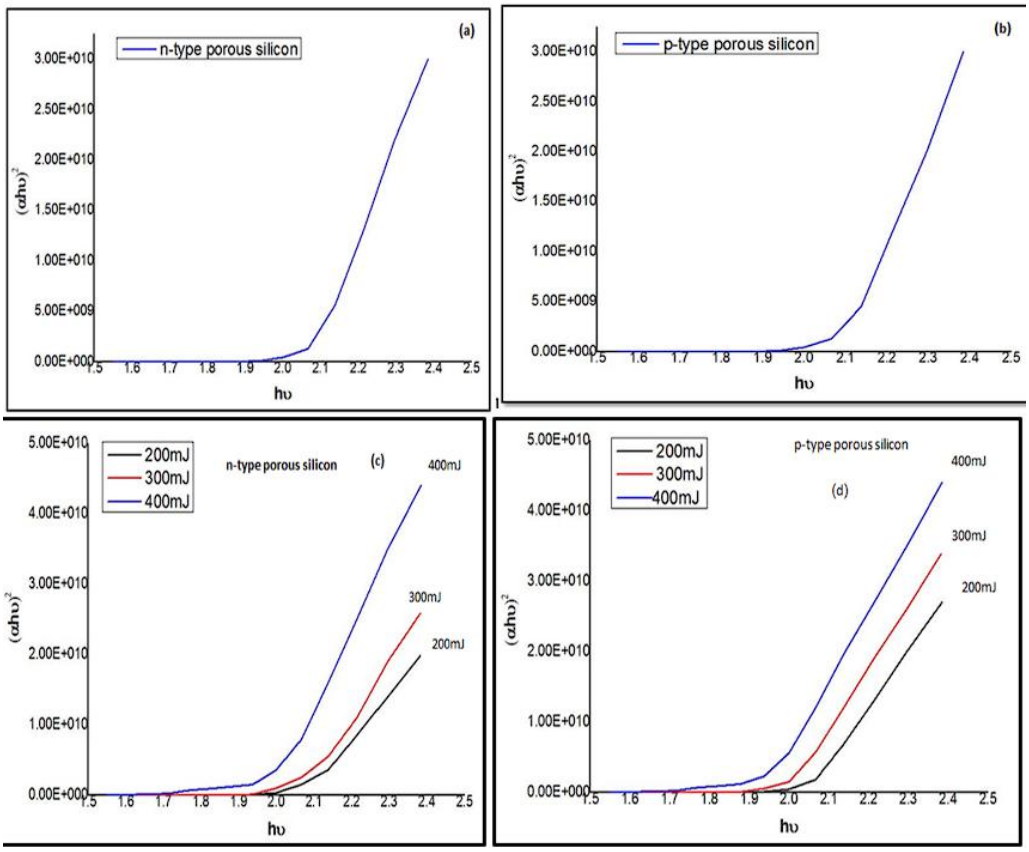

Figure 6 Energy gap of AuNPs/PSi (a) pre- n-type PSi (b) pre- p-type PSi (c) n-type PSi after laser ablation (d) p-type porous silicon after laser ablation.

Table 1 Laser energy, strong absorption peak and energy gap of Au nanoparticles.

Laser energy (mJ)	Strong absorption peak	Wavelength (nm)	Crystalline size (A°)
200	0.42	542	2.11
300	0.66	546	2.14
400	0.83	550	2.19

Photoluminescence (PL) measurements

Figure 7 shows the PL spectra of gold nanoparticles deposited on PSi at different laser energy (200, 350 and 400 mJ). PL spectra exhibited different peak positions due to the different sizes of Au nanoparticle. However, the PL intensity decreased with laser power owing to the free electrons as well as the presence of SPR spectrum which was enhanced the electromagnetic field close the gold nanoparticles. Plasmon resonance may be attributed to the quantum size effect from the Au nanostructure [24]. The recombination centers are formed by Si atoms at the layer of crystallite and angles to accommodate changes in local condition [25]. Furthermore, the full width (FWHM) of porous silicon is increased after laser ablation and after embedding of Au nanoparticles on the PSi. This can enhance the spectral detection of optical PSi towards the red-band region. This results agree with results found by [26]. The diameter size increases with laser power. The values of energy gap can be determined by [27]:

$$Eg^* = Eg + \frac{88.34}{D^{1.37}} \quad (2)$$

where Eg^* symbolizes the energy gap of porous silicon, Eg refers to the bandgap of bulk Si and D refers the crystallite size. The values of energy gap (Eg*) was 2.19 eV for n-type and as 2.22 eV of p-type silicon. These results were consistent with UV-Visible measurements. The results are presented in **Table 2**.

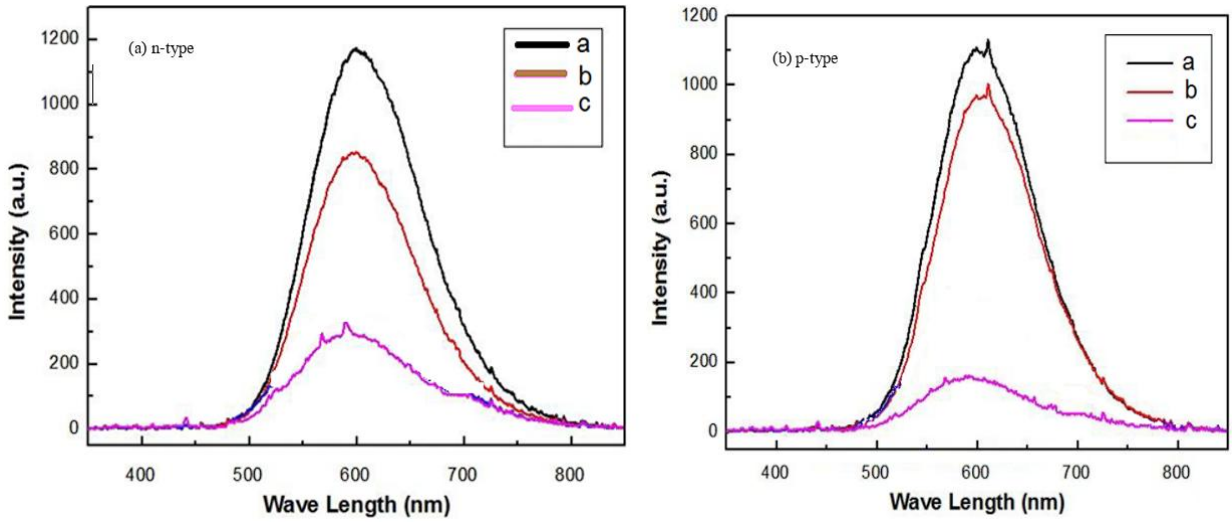

Figure 7 PL patterns of AuNPs/PSi of n-type and p-type PSi; (a) 200 mJ, (b) 300 mJ, (c) 400 mJ.

Table 2 Parameters of crystallite size, peak position values and energy gap of PSi for laser power of 200, 300 and 400 mJ for n-type and p-type PSi.

Sample	laser power (mJ)	peak position (nm)	Crystalline size (A°)	Eg (eV)
n-type PSi	200	583	2.73	2.12
	300	587	2.75	2.11
	400	593	2.78	2.09
p-type PSi	200	570	2.69	2.17
	300	576	2.70	2.15
	400	580	2.72	2.13

Electrical properties of AuNPs/PSi

The electrical properties (I-V) curves of AuNPs/PSi sample have been studied for different laser energy (200, 300 and 400 mJ). The I-V characteristics were achieved in dark by applying a forward bias DC voltage (from 0 to 6 V). (**Figures 8** and **9**) reveal a typical diode performance of the (I-V) curve. The results show rectifying behavior due to the formation of hetero-junction between Au nanoparticles and porous silicon layer interface, this junction is called Schottky junction [28]. The distinguish between pre- porous silicon substrate and after deposition of Au nanoparticles samples, the first region at low voltages for forward bias the porous silicon has small values of current compared to AuNPs/PSi due to the higher Eg corresponding to the quantum confinement. It is clear, the recombination between excited electrons and holes is large due to insufficient energy for electrons to overcome the deeper barrier also the formation of capture centers which is formed from the porous structure of porous silicon. This is due to an increase of resistivity and then reduce in the amount of current flow at the surface [29]. Furthermore, the second region at higher voltage show that the current increases rapidly with the applied voltage after laser ablation due to exceeding the potential barrier. This voltage provides the electron enough energy to overcome the deeper barrier and that is what called diffusion current as it is shown in **Figure 10**. **Tables 3** and **4** present the important parameters calculated from I-V measurements of AuNPs/Psi. It is observed that the electrical properties of the samples are improved when the laser power values are increased. These results agree with Khalifa *et al*. [30].

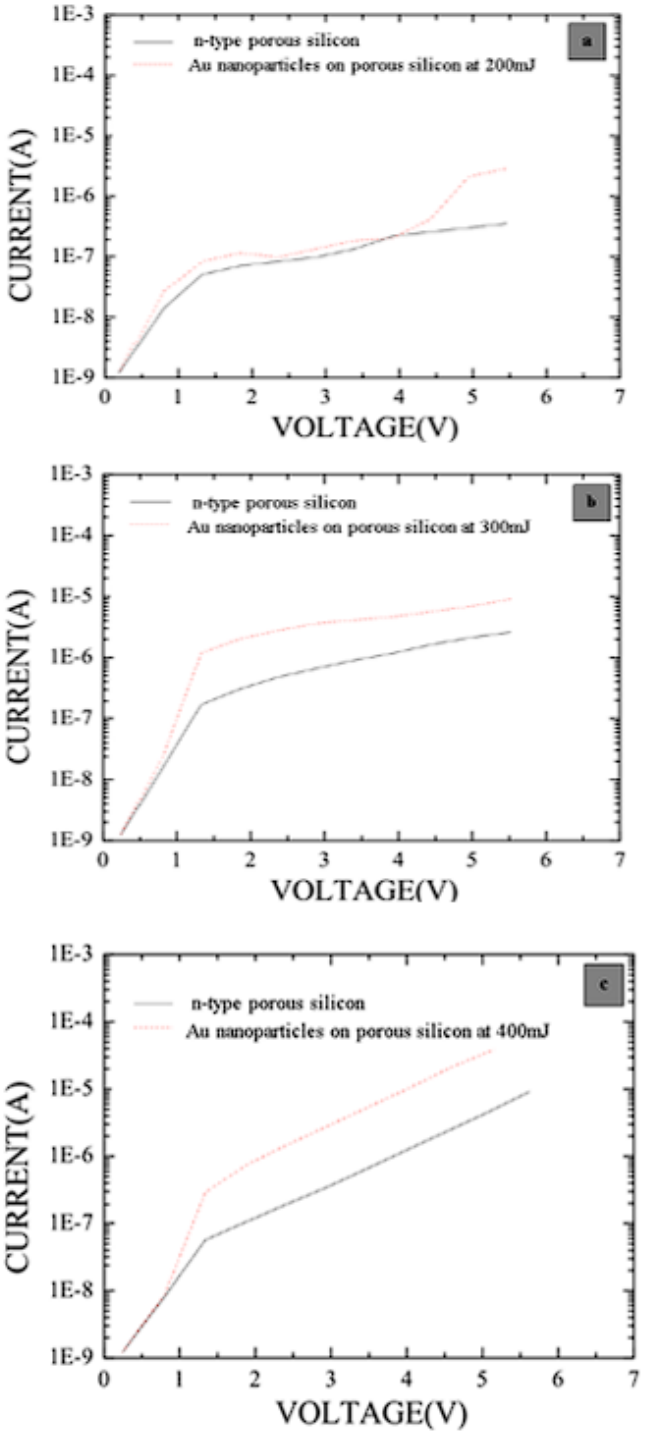

Figure 8 I-V curves of gold nanoparticles deposed on PSi n-type of laser ablation; (a) 200 mJ, (b) 300 mJ (c) 400 mJ.

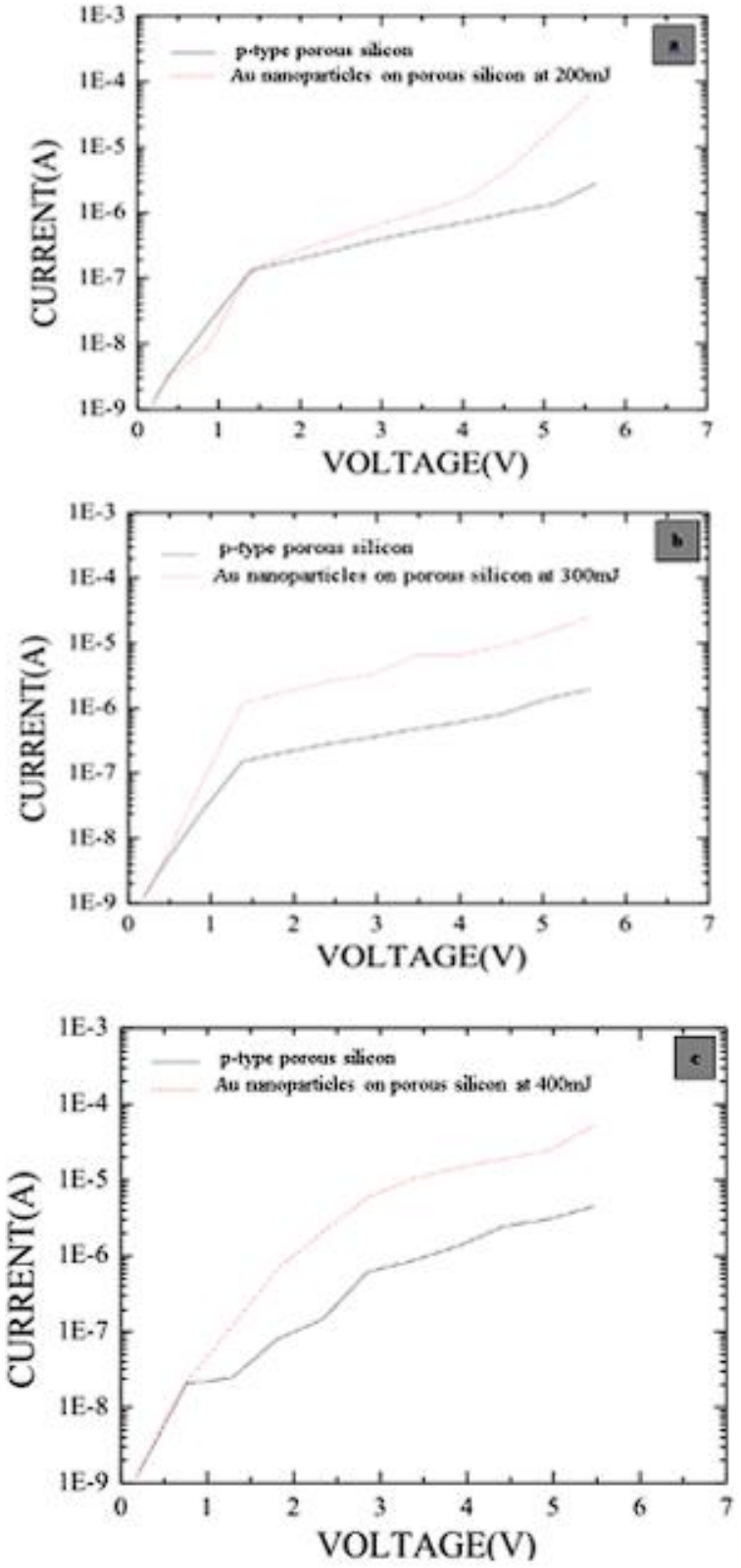

Figure 9 I-V curves of Au nanoparticles on porous silicon p-type of laser ablation at (a) 200 mJ, (b) 300 mJ (c) 400 mJ.

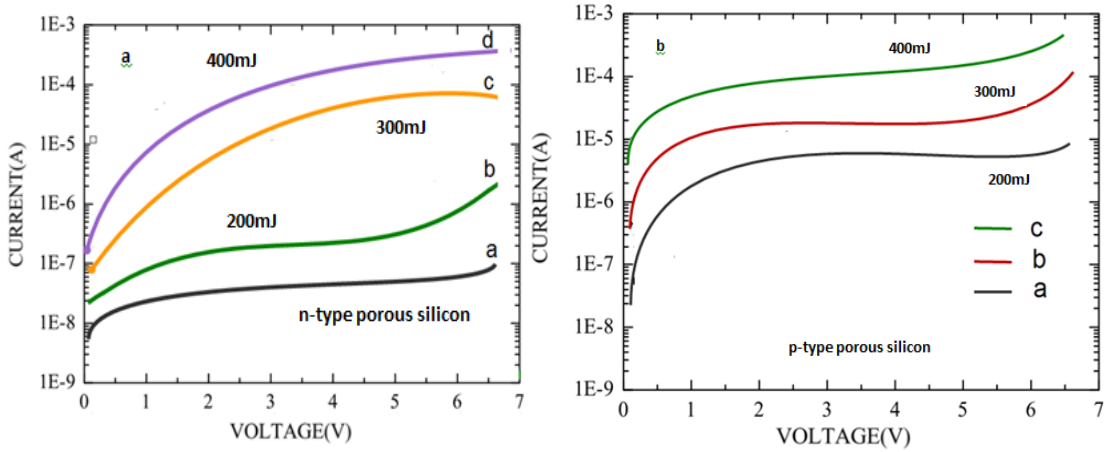

Figure 10 I-V curves of of gold nanoparticles deposed on PSi of laser ablation at 200, 300 and 400 mJ; (a) n-type porous silicon (b) p-type porous silicon.

Table 3 Parameters of AuNPs/PSi at etching time 30min before and after laser ablation of n-type porous silicon.

Sample n-type	Laser energy(mJ)	J_s (mA/cm^2)	n	φ (eV)	(Ω.cm)ρ
PSi	-	0.0003	2.93	0.727	3.45×10^{8}
AuNPs/PSi	200	3.52	2.77	0.672	5.26×10^{6}
	300	8.56	2.73	0.643	7.2×10^{5}
	400	11.56	2.68	0.621	5.4×10^{4}

Table 4 Laser energy, Parameters of AuNPs/PSi at etching time 30min before and after laser ablation of p-type porous s icon.

Sample p-type	Laser energy(mJ)	J_s (mA/cm^2)	n	φ (eV)	(Ω.cm)ρ
PSi	-	0.004	2.88	0.71	1.85×10^{7}
AuNPs/PSi	200	3.52	2.75	0.654	3.26×10^{6}
	300	15.56	2.71	0.633	4.3×10^{5}
	400	34.56	2.65	0.61	2.65×10^{4}

Conclusions

We deposited Au nanoparticles on both n-type and p-type porous silicon samples by laser ablation technique to create AuNPs/PSi materials at various laser power (200, 300 and 400 mJ). All samples were tested by high resolution scanning electron microscope (SEM), UV-spectrophotometer, Photoluminescence (PL) and I-V characteristics. The results showed a considerable impact of the laser ablation energy, on the optical and electrical properties on the gold nanoparticles on PSi. The results indicate that the absorption spectra increase with increasing laser power, The photoluminescence of gold nanostructures revealed the peak position was shifted to the long wavelength (redshift) with increasing energy. The electrical properties of AuNPs/PSi enhanced with increasing laser power. In brief, Au nanoparticles on PSi showed a high capability due to the high lattice match between them. additionally, there is an improvement in electrical and optical characteristics of the AuNPs/PSi structure, hence, offer the potential of optimization the performance of porous silicon.

Acknowledgments

The authors thank college of education for pure science, Mosul University, Iraq for their logistic support.

References

[1] K Alaqad and TA Saleh. Gold and silver nanoparticles: Synthesis methods, characterization routes and applications towards drugs. *Journal of Environmental & Analytical Toxicology* 2016; **6(4)**, 2161-0525.

[2] RM Ibrahim and MS Mohammed. Effect of material irradiated type and spot size on spot center temperature of a diode-pumped solid state laser. *Iraqi Journal of Applied Physics* 2024; **20(3)**, 540-544.

[3] RM Ibrahim and IB Karomi. Effect of tapered length on operation of traveling-wave semiconductor laser amplifier: A numerical study. *Iraqi Journal of Applied Physics* 2024; **20(4)**, 769-774.

[4] OA Alhamd, GG Ali and MSH Aljuboori. Study and characterization of copper and titanium oxides nanostructures for some molecular and biological applications. *Trends in Sciences* 2024; **21(4)**, 7402.

[5] MH Younus, GG Ali and HA Salih. The reinforced optical fiber sensing with bilayer AuNPs/SiC for pressure measurement: Characterization and optimization, *Journal of Physics: Conference Series* 2021; **1795**, 012002.

[6] P Prema and S Thangapandiyan. *In-vitro* antibacterial activity of gold nanoparticles capped with polysaccharide stabilizing agents. *Journal of Pharm Science* 2013; **5(1)**, 310-314.

[7] C Gonzalez, RG Eugenio, JV Ernesto, LC Carlos and AA Jacob. Assisted laser ablation: Silver/gold nanostructures coated with silica. *Journal Applied of Nano Science* 2017; **7**, 597-605.

[8] S Francisco. Potential of porous silicon doped with gold nanoparticles in detection of biogenic amine. Porous silicon used in the detection of biogenic amines. *Glob Journal of Nanomedicine* 2017; **1(2)**, 345-357.

[9] K Fukami, L Mohamed, R Miyagawa, AN Munoz, T Sakka and MS Manso. Gold nanostructures for surface - enhanced raman spectroscopy prepared by electro-deposition in porous silicon. *Journal of Materials* 2011; **4(2)**, 791-800.

[10] TST Amran, MR Hashim, NKA Al-Obaidi, H Yazid and R Adnan. Optical absorption and photoluminescence studies of gold nanoparticles deposited on mesoporous silicon. *Nanoscale Research Letters* 2013; **8(1)**, 35.

[11] FA Mytlak, MS Jabir, UM Naif and HI Fadhil. Synthesis and characterization of Au nanoparticles for nanomedicine application. *Iraqi Journal of Physics* 2017; **15(35)**, 109-116.

[12] M Uday and M Intisar. Synthesis of gold nanoparticles by laser ablation on porous silicon for sensing CO_2 gas. *Iraqi Journal of Physics* 2018; **16(36)**, 1-10.

[13] I Khalil, CM Chou, KL Tsai, S Hsu, WA Yehye and VKS Hsiao. Gold nanofilm-coated porous silicon as surface-enhanced raman scattering substrate. *Applied Sciences* 2019; **9(22)**, 4806.

[14] M Kim, S Osone, T Kim, H Higashi and T Seto. Synthesis of nanoparticles by laser ablation: A review. *Journal of Materials* 2017; **34**, 80-90.

[15] GG Ali, AKA Sulaiman and IB Karomi. The effect of the ZnO thickness layer on the porous silicon properties deposited by chemical vapor deposition. *AIP Conference Proceedings* 2018; **2034**, 020009.

[16] GG Ali, MA Ahmed and AA Sulaiman. Structural properties of AuNPs/PSi nanostructure. *Digest Journal of Nanomaterials and Biostructures* 2022; **17(2)**, 473-480.

[17] W Chen, W Cai, L Zhang, G Wang and L Zhang. Sonochemical processes and formation of gold nanoparticales within pores of mesoporous silicon. *Journal Colloid and Interface Science* 2001; **238(2)**, 291-295.

[18] A Kumar, VL Pushparaj, S Murugesan, G Viswanathan, R Nalamasu, RJ Linhardt, O Nalamasu and PM Ajayan. Synthesis of silica-gold nanocomposites and their porous nanoparticles by an in-situ approach. *American Chemical Society* 2006; **22(21)**, 8631-8634.

[19] N Mirghassemzadeh, M Ghamkhari and D Dorranian. Dependence of laser ablation produced gold nanoparticles characteristics on the

fluence of laser pulse. *Soft Nanoscience Letters* 2013; **3(2)**, 101-106.

[20] AA Ahmed, GG Ali, NA Daham. Performance of high sensitive heterojunction CuS/porous silicon photodetector. *Chalcogenide Letters* 2024; **21(1)**, 81-97.

[21] R Jarimaviciute-Zvalionienea, I Prosycevasa, Z Kaminskienea and S Lapinskas. Optical properties of black silicon with precipitated silver and gold nanoparticles. *Journal of Acta Physica Polonica* 2011; **120(5)**, 144-154.

[22] RA Ismail, NJ Almashhadani and RH Sadik. Preparation and properties of polystyrene incorporated with gold and silver nanoparticles for optoelectronic applications. *Journal of Applied Nanoscience* 2017; **7**, 109-116.

[23] M Bassu, ML Strambini, G Barillaro and F Fuso. Light emission from silicon/gold nanoparticle systems. *Applied Physics Letters* 2010; **97**, 143113.

[24] K Chan, BT Goh, SA Rahman, MR Muhamad, CF Dee and Z Aspanut. Annealing effect on the structural and optical properties of embedded Au nanoparticles in silicon suboxide films. *Vacuum* 2012; **86**, 1367-1372.

[25] AG Cullis, LT Canham and PDJ Calcott. The structural and luminescence properties of porous silicon. *Journal of Applied Physics* 1997; **82**, 909-965.

[26] AV Skobelkina, FV Kashaev, AV Kolchin, DV Shuleiko, TP Kaminskaya, DE Presnov, LV Golovan and PK Kashkarov. Silicon nanoparticles formed via pulsed laser ablation of porous silicon in liquids. *Journal of Technical Physics Letters* 2020; **46**, 687-690.

[27] K Behzad, WM Yunus, ZA Talib, A Zakaria and A Bahrami. Preparation and thermal characterization of annealed gold coated porous silicon. *Materials* 2012; **5(1)**, 157-168.

[28] ZJ Abdulkareem, M Uday, UM Nayef, A Kadhim and KA Hubeatir. Investigation of laser assisted etching for preparation silicon nanostructure and diagnostic physical properties. *Engineering and Technology Journal* 2015; **33(4)**, 595-601.

[29] GG Ali, IB Karomi, AA Sulaiman and AM Mohammed. Properties of p-type porous silicon bombarded by neutrons. *Nuclear Instruments and Methods in Physics Research Section B: Beam Interactions with Materials and Atoms* 2020; **468**, 23-27.

[30] MJ Khalifa, MH Jaduaa and AN Abd. Quantum dots gold nanoparticle/porous silicon/silicon for solar cell applications. *Journal of Nanostructure* 2020; **10(4)**, 863-870.